Original Article

American Cleft Palate–Craniofacial Association

The Cleft Palate-Craniofacial Journal
1-12

DOI: 10.1177/1055665620954321
journals.sagepub.com/home/cpc
SAGE

Effectiveness of a Novel 3D-Printed Nasoalveolar Molding Appliance (D-NAM) on Improving the Maxillary Arch Dimensions in Unilateral Cleft Lip and Palate Infants: A Randomized Controlled Trial

Mohamed Abd El-Ghafour, BDS, MSc, PhD, MOrth RCSEd[1], Mamdouh A. Aboulhassan, MD[2], Mona M. Salah Fayed, BDS, MSc, PhD[1], Amr Ragab El-Beialy, MSc, PhD, MOrth RCSEd[1], Faten Hussein Kamel Eid, BDS, MSc, PhD[1], Seif El-Din Hegab, BDS, MSc, MOrth RCSEd[1], Mahmoud El-Gendi, BDS[1], and Dawlat Emara, MD[3]

Abstract

Objective: The aim of the current study was to introduce and measure the effectiveness of a new 3D-printed nasoalveolar molding (D-NAM) appliance on improving the maxillary arch dimensions (MADs) in infants with unilateral complete cleft lip and palate (UCLP) before surgical lip repair.

Design: A prospective, balanced, randomized, parallel groups, single-blinded, controlled trial.

Setting: All the steps of the current study were carried in the Department of Orthodontics, Cairo University in Egypt.

Participants: Thirty-four, nonsyndromic infants with UCLP.

Interventions: The eligible infants were randomly assigned into either no-treatment (control) or to the new D-NAM groups. In D-NAM group, the maxillary models were 3D scanned into virtual models onto which segmentation and alveolar segments approximation were performed. Approximation movements were divided into 3 models representing 3 activation steps. On each of these models, virtual appliance construction was performed followed by 3D printing of the appliance. Nasal stent was added manually to the appliances of the second and third steps. Horizontal tapes were applied to infants in the D-NAM group only.

Main Outcomes Measures: A Blinded assessors carried all the MADs measurements virtually on digital models collected at the beginning (T1) and after (T2) treatment.

Results: Clinically and/or statistically significant improvements in all the measured MADs were recorded in D-NAM group at T2 before surgical lip repair in comparison to control group.

Conclusions: The introduced D-NAM/3D-printed appliance is a simple and efficient technique to improve the MADs in infants with UCLP before surgical lip repair.

[1] Department of Orthodontics, Faculty of Dentistry, Cairo University, Cairo, Egypt
[2] Department of Pediatric Plastic Surgery, Faculty of Medicine, Cairo University, Cairo, Egypt
[3] Department of Plastic Surgery, Faculty of Medicine, Cairo University, Cairo, Egypt

Corresponding Author:
Mohamed Abd El-Ghafour, Royal College of Surgeon Edinburgh, UK; American Cleft Palate-Craniofacial Association (ACPA); Department of Orthodontics, Faculty of Dentistry, Cairo University, Egypt; Department of Orthodontics, Faculty of Dentistry, Cairo University, 11 El-Saraya Street, Manial, Cairo Egypt.
Email: m.abdelghafour@dentistry.cu.edu.eg

Keywords
cleft lip and palate, nasoalveolar molding, computer-aided design, 3D-printing

Introduction

Cleft lip and palate (CLP) is considered the most common craniofacial anomaly in different populations (Mossey and Modell, 2012). Patients with CLP have several problems: functional (Breitsprecher et al., 1999; Gkantidis et al., 2015), pathologic (Hocevar-Boltezar et al., 2006; Zhu and Chen, 2013), social (Schimming et al., 1999; van der Plas et al., 2013; Gkantidis et al., 2015), and aesthetic (Schimming et al., 1999; Hocevar-Boltezar et al., 2006; Gkantidis et al., 2015). The amount of cleft gap between the lip segments and the collapse in the nasal cartilage affect the final aesthetic result of the surgical closure of the lip and nose (Rousseau et al., 2013; Campbell et al., 2019). The wider the cleft gap between the alveolar segments, the more tension will be produced on the surgical wound. Similarly, the wider the cleft gap the more collapse will occur to the nose. In addition to the unsatisfactory aesthetic result of the surgery, the tension produced from the lip results in restriction of the maxillary growth and retroclination of the premaxilla (Friede and Lilja, 1994; Lisson et al., 1999).

The idea of Presurgical Infant Orthopedics (PSIO) started as a procedure that could be done early before the surgical lip closure aiming in decreasing the cleft gap width and improve nose aesthetics (Ross and MacNamera, 1994). Presurgical Infant Orthopedics started in 1686 by trials to retract protrusive premaxilla in patients with bilateral CLP (Hoffman, 1686). In 1844, Hullihen used adhesive tape to stretch the lip segments to decrease the distance between them. In 1927, Brophy (1923) had used silver wires to approximate the alveolar segments before surgical lip repair, then McNeil (1956) used an appliance to direct the arch segments before lip correction. Latham et al. (1976) in 1976 invented a presurgical appliance which was retained by pins inserted in the alveolar ridge to approximate the ridge segments.

All the mentioned trials were directed to correct the ridge and lip only until Grayson et al. (1993) in 1993 added a nasal stent to the intraoral plate to mold the nasal cartilage into a normal form, such an appliance was named the nasoalveolar molding (NAM). The authors were inspired by a study by Matsuo et al. (1984) in 1984 who was able to mold a deformed auricular cartilage by a similar acrylic stent. Based on that concept, Grayson thought that it could be done for the nasal cartilage. Hence, the aim of the PSIO is to approximate the alveolar and lip segments and to improve the nasal aesthetics before surgical lip closure to achieve better results after surgery.

In 2006, another technique of NAM was introduced by Figueroa and Polley (2006). They used an intraoral plate made of light-cured acrylic resin. They attached to the intraoral plate a nasal stent with a loop on its wire for future adjustments. Similar to Grayson's NAM, they did selective grinding and addition of acrylic in specific parts of the plate allowing for narrowing of the alveolar cleft before surgery (Gomez et al., 2012). They didn't use the extraoral tapes nor the elastics, that's why they removed the acrylic button. Tapes were used only for the severe cases and they retained the appliance in place using denture adhesives. In a comparison between the 2 techniques (Grayson's and Figueroa's), no differences were found in the assessed results as concluded by a randomized clinical trial done by Chang et al. (2014) in 2014.

Recently, the era of "digital orthodontics" is invading the profession and it seems that the NAM was not missed in this new paradigm. Digital activation of the NAM appliances was introduced by Yu et al. (2011) in 2011 under the name of "computer-aided design/nasoalveolar molding" (CAD/NAM). In this technique, a software was used to produce a series of 3D-printed models encompassing the sequence of the activation steps. On these physical models, a set of appliances were manually constructed for each patient. Thereafter, more studies (Gong and Yu, 2012; Yu et al., 2013; Loeffelbein et al., 2015; Shen et al., 2015; Ritschl et al., 2016) were published testing the same concept on different samples.

The aim of the current randomized controlled trial (RCT) is to introduce a new technique of CAD/NAM, where the appliances were virtually constructed and 3D printed (unlike the available technique of 3D printing the models and manual appliance construction). Subsequently, to measure the effectiveness of the introduced technique in improving the maxillary arch dimensions (MADs) in infants with unilateral complete cleft lip and palate (UCLP) before surgical lip repair.

Materials and Methods

The current RCT followed the CONSORT (Consolidated Standards of Reporting Trials) guidelines (Moher et al., 2010) for reporting RCTs allowing detailed description of the study interventions and assessment methods.

Trial Design and Registration

The current study was conducted in a balanced, randomized, parallel groups, single-blinded, controlled trial design which conducted in Egypt. Single large group of participants with matching baseline characteristics was randomly divided into 2 parallel groups with allocation ratio 1:1. The 2 groups were the Digital NAM group (D-NAM) and the other group was no treatment controls. Trial registration was done in ClinicalTrials.gov with registration number of: NCT02845193. The trial's protocol was registered on July 27, 2016. The protocol

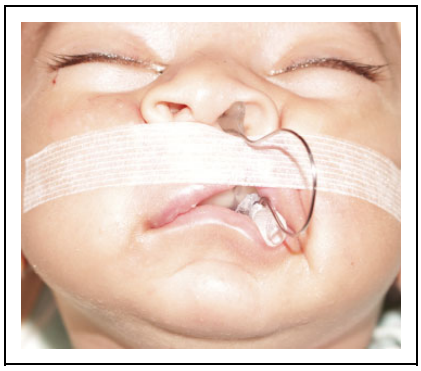

Figure 1. The 3D-printed nasoalveolar molding (D-NAM) in place with the nasal stent and the horizontal taping.

can be accessed through: https://clinicaltrials.gov/ct2/show/NCT02845193. The study was reviewed and approved by the ethics committee of the Faculty of Dentistry, Cairo University, and its whole process was supervised.

Participants

Thirty-four infants with complete UCLP were recruited in the current study. All the recruited patients followed the inclusion criteria of infants with age range from 1 to 30 days, unilateral complete cleft lip and alveolus, presence of complete cleft palate, medically free patients, and both males and females were included.

All the steps of the current RCT were performed by the principal operator (M.A.) in the outpatient clinic of the Department of Orthodontics, Faculty of Dentistry, Cairo University.

Interventions

Upon receiving a new infant (at T1: before starting any treatment), 2-step rubber-based maxillary impression was made. Rubber-based impression material (Zetaplus-Zhermack Putty and light) was used with 2 different viscosities: putty and light. All the impressions were made using an acrylic impression tray made on previous models. The made impression was poured with hard stone. At T2 (after NAM treatment and before surgical lip repair), another maxillary impression was made to all the included infants in the both groups. Infants of the control group did not receive any intervention but the 2-maxillary impressions at T1 and T2.

In the D-NAM group, the included infants received a single horizontal tape (3M Steri strips-1/4 Inch) stretching the 2 labial segments toward each other, aiming to decrease the interlabial gap. The parents were instructed to place the tape 24 h/d and to be changed everyday (Figure 1). If any inflammation occurred to the skin the parents were instructed to use an aerobic batch of tape. They were instructed to change it every 2 to 3 days. It acted as a base for the Steri-strips to be changed without further skin irritation.

All the steps of the D-NAM construction including models' scanning, activation movements, and virtual appliance construction were done by the principal operator. The produced model passed through the following steps till reaching the final appliance.

Model scanning. The produced model was scanned with the desktop scanner (3shape Lab Scanner-R500) and a software (3shape Scan-it Manager) aiming to produce the virtual model. The virtual model was produced not watertight by default. In order to produce a watertight model, virtual model base was constructed for each model.

Model segmentation and modification. Using a desktop software (3shape Ortho Analyzer), model segmentation and modification was performed. The maxillary model was divided into 3 segments: premaxillary segment in the middle and 2 right and left posterior segments (Supplemental Video 1). This was done to facilitate model modification and allow easy movements of the different parts to close the cleft gap.

The 3 segments were positioned in the desired directions and adjusted using a control panel until reaching the required arch form. By hitting the button of treatment simulation, the 3 selected segments were free to move to the needed direction to close the cleft gap (Supplemental Video 2).

The produced movements were divided into 3 sequencing steps. After each 1/3 of the movements (ie, one step), a new model was produced (Figure 2). On each model, a new appliance was constructed, that is, each patient supposed to receive a series of 3 appliances. Then, the 3 models (Figure 2) were exported to be used in the next module.

Virtual appliance construction. Virtual appliance construction was done using another module of the same software (3shape Appliance Designer). After selection of the needed model, the task of *Add* "modify model" was selected. By using this tool, addition was done in the cleft and relief areas till complete obliteration of the cleft gap. The removal tool was used to remove layers from the model at the pressure areas.

Then, the undercut obliteration button was selected to automatically obliterate any undercuts that might interfere with appliance construction, insertion or removal. First, the path of insertion was selected, then the amount of retention set to be 0.1 mm, automatic conversion of the model to undercut free version was performed by the software.

On the undercut free model, the intraoral plate was constructed. By selection of shell construction button, the pass of insertion was selected, then the plate thickness was adjusted to be 2 mm. The borders of the appliance were identified using the splines (Supplemental Video 3). Then, the final appliance was virtually constructed (Supplemental Video 3). After plate construction, the button was virtually added and adjusted to the desired place (Supplemental Video 3). The constructed appliance was then exported in stereolithographic (STL) format and sent for 3D printing. All the previous steps were repeated for each of the 3 models to produce a series of 3 appliances

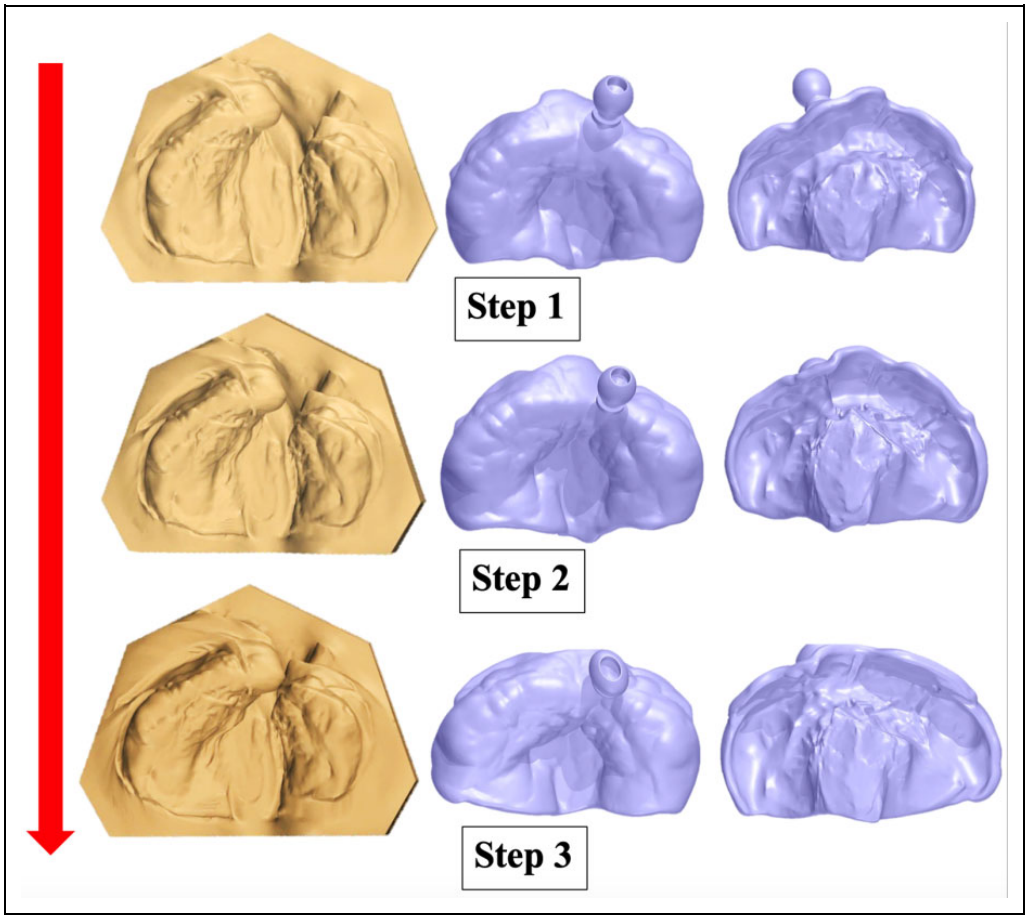

Figure 2. The 3 virtually activated steps; the activated models (left) and the virtually constructed appliances (right).

(Figure 2). Each step was used for a nearly one month, then followed by the next step until reaching the third appliance. In most of the cases, the followed steps consumed 20 to 30 minutes per patient to produce the STL files of the 3 virtual intraoral plates.

3-dimensional printing. The extracted STL file was sent to the laboratory to be printed by the stereolithography technique (ZENITH U 3D printer, Desktop system for universal use). The material used was light curable acrylic resin suitable for the used 3D printer (NextDent Ortho Rigid, Vertex-Dental). Using the printer's software supports were added virtually to the appliance to allow proper printing process. When the supports were ready, printing process started to produce the final appliance (Figure 3).

Nasal stent addition and appliance insertion. The nasal stent was made using stainless steel wrought round wire with diameter of 0.8 mm. The wire was bent starting with a loop (as a mean of retention to the intraoral plate), then a curved part "the swan neck" (5-cm long), then a kidney-shaped loop. This kidney-shaped loop was covered with acrylic resin to act as a stent to mold the nasal cartilage (Figure 1). The nasal stent was fixed manually to the 3D-printed intraoral plate using self-cured acrylic resin. The nasal stent was added manually when the cleft gap was 5 mm or less, this was usually occurred while using the appliance of the second step.

The appliance was fixed in place using denture adhesive (Corega cream [gsk- GlaxoSmithKline]) to retain the appliance. A small amount of the denture adhesive was added on the appliance's fitting surface, then held it in place till complete setting and appliance retention. Follow-up visits were every 2 weeks for 3 months.

Outcomes

The outcome of this RCT was to measure the effectiveness of the D-NAM in improving the maxillary arch changes in comparison to control group of infants with UCLP. This was assessed as the difference between T1 (at the start of the treatment) and T2 (after D-NAM treatment and before surgical lip closure at nearly 3 months of age). All the T1 and T2 models were scanned using desktop scanner (3shape Lab Scanner-R500) upon which all the landmarks were identified and measurements were carried out. Using a software (3shape Ortho Control Panel), a custom analysis was constructed including landmarks, lines, and distances

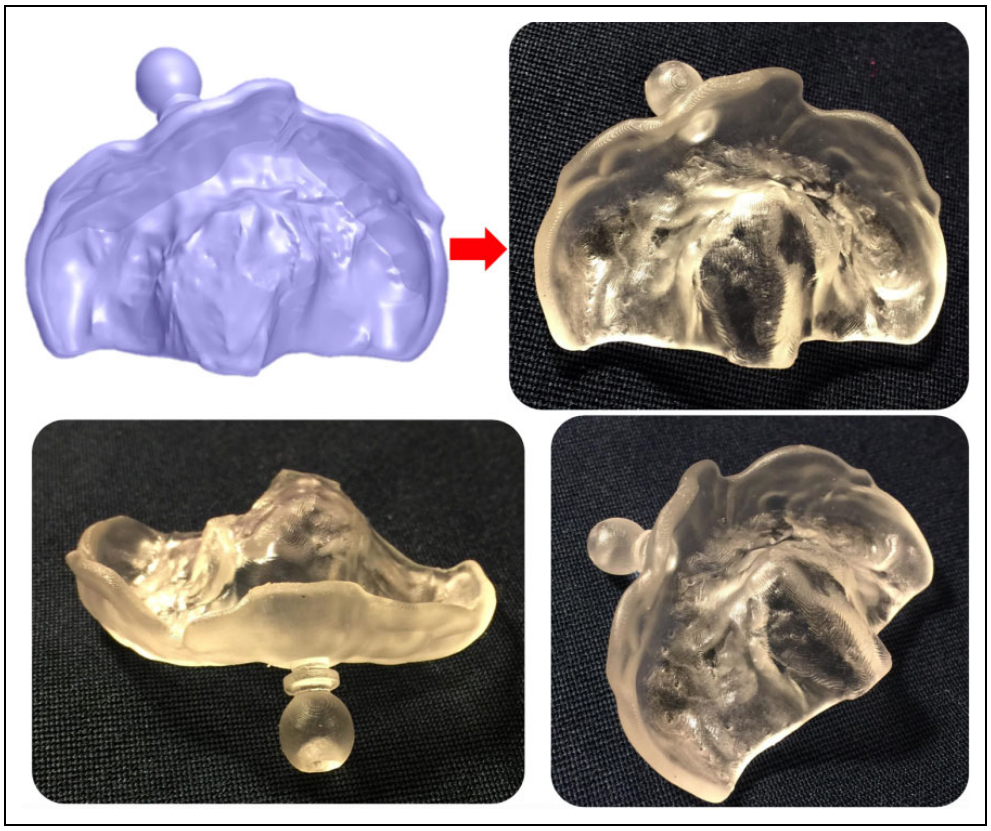

Figure 3. The 3D-printed intraoral plate.

mentioned in Table 1 and Figure 4. Landmarks identification was completed using the measuring module in the used software (3shape Ortho Analyzer). After landmark identification, the software automatically generated the aforementioned measurements.

Sample Size

Calculation of the sample size was done using data from previous similar study (Yu et al., 2013), which used another technique of the CAD/NAM. Mean and standard deviation of the anterior cleft gap of the intervention group were used. By setting the power of 80 %, type I error of 5% and using independent sample *t* test, effect size of 1.59 resulted. The calculation donated the inclusion of 8 infants in each group. In the current trial, this number was increased to 17 in each group to avoid any dropouts and to prevent the attrition bias.

Randomization

Randomization process was strictly followed by applying its 3 steps. Starting with sequence generation using Microsoft Office Excel 2013 sheet, followed by allocation concealment by writing the random numbers on opaque white papers, each was folded 8 times and kept in opaque sealed envelopes, then kept in 15 × 15 cm sealed box till time of implementation. Finally, implementation was performed by blinded implementer upon receiving a new eligible infant to identify his/her allocation group.

Blinding

The current trial is considered as a single-blinded study, blinding was done only to the outcome assessors. The first assessor was responsible for placing the landmarks on all the digital models, and repeat 20 % of the measurements after 2 weeks to measure the intraobserver reliability. The second assessor placed the landmarks on the same 20% of the sample to measure the interobserver reliability. Due to the nature of the intervention, it was impossible to blind both the patients and the principal operator.

Statistical Methods

The significance level was set at $P \leq .05$. Statistical analysis was performed with IBM SPSS Statistics Version 20 for Windows. Handling of data was done using Microsoft Excel software.

Interclass correlation coefficients (ICCs) were calculated to detect the intra- and interobserver reliability of the measurements in the study. The closer the ICC to 1.0, the higher was the reliability of the measurement.

Table 1. Definition of Landmarks and Measurements.

	Landmarks		
	Landmark	Abbreviation	Definition
1	Greater segment anterior point	G	The anterior end of the greater segment along the crest of the alveolar ridge.
2	Lesser segment anterior point	L	The anterior end of the lesser segment along the crest of the alveolar ridge.
3	Incisive point	I	The intersection of the crest of the alveolar ridge and line drawn from the labial frenum to the incisive papilla.
4	Canine point of the greater segment	C	The intersection of the anterolateral sulcus and the crest of the alveolar ridge of the greater segment.
5	Canine point of the lesser segment	C'	The intersection of the anterolateral sulcus and the crest of the alveolar ridge of the lesser segment.
6	Gingival groove point of the greater segment	Q	The intersection between the gingival groove (junction between attached gingival and alveolar mucosa) and the anterolateral sulcus of the greater segment.
7	Gingival groove point of the lesser segment	Q'	The intersection between the gingival groove (junction between attached gingival and alveolar mucosa) and the anterolateral sulcus of the lesser segment.
8	Tuberosity point of the greater segment	T	The posterior limit of the crest of the alveolar ridge of the greater segment.
9	Tuberosity point of the lesser segment	T'	The posterior limit of the crest of the alveolar ridge of the lesser segment.
	Constructed Points		
	Point	Abbreviation	Definition
1	Canine palatal point of the greater segment	c	The point at the intersection between C-C' line and cleft margin of the greater segment.
2	Canine palatal point of the lesser segment	c'	The point at the intersection between C-C' line and cleft margin of the lesser segment.
3	Middle palatal point of the greater segment	m	The intersection of cleft margin and a line connecting points C and Q on the greater segment.
4	Middle palatal point of the lesser segment	m'	The intersection of cleft margin and a line connecting points C' and Q' on the lesser segment.
5	Posterior palatal point of the greater segment	t	The point at the intersection between T-T' line and cleft margin of the greater segment.
6	Posterior palatal point of the lesser segment	t'	The point at the intersection between T-T' line and cleft margin of the lesser segment.
7	Point Z	Z	Point of intersection of perpendicular line from point I to T-T' line.
8	Point F	F	Point of intersection of perpendicular line from point I to C-C' line.
9	Point Y	Y	Point of intersection of perpendicular line from point G to T-T' line.
10	Point N	N	Point of intersection of perpendicular line from point L to T-T' line.
11	Point X	X	Point of intersection of perpendicular line from point L to GY line.
12	Point E	E	The point at the intersection between LX line and cleft margin of the greater segment.
13	Point O	O	Mid-line point on T-T' line.
	Measurements		
	Measurement	Abbreviation	Definition
	I] Cleft Widths:		
1	Anterior cleft width	ACW (G-L)	Distance between points G and L.
2	Canine cleft width	CCW (c-c')	Distance between points c and c'.
3	Middle cleft width	MCW (m-m')	Distance between points m and m'.
4	Posterior cleft width	PCW (t-t')	Distance between points t and t'.
	II] Arch Widths:		
5	Intercanine region width	ICW (C-C')	Distance between points C and C'.
6	Middle arch width	MAW (Q-Q')	Distance between points Q and Q'.
7	Posterior arch width	PAW (T-T')	Distance between points T and T'

(continued)

Table 1. (continued)

	Landmarks		
	Landmark	Abbreviation	Definition
	III] Anteroposterior Measurements:		
8	Greater segment position	GSP (GY)	Distance between points G and Y.
9	Greater segment length	GSL (G-C-T)	Distance between points G and C plus distance between points C and T.
10	Lesser segment position	LSP (LN)	Distance between points L and N.
11	Lesser segment length	LSL (LT')	Distance between points L and C' plus distance between points C' and T'.
12	Anterior arch length	AAL (IF)	Distance between points I and F.
13	Total arch length	TAL (IZ)	Distance between points I and Z.
14	Greater to lesser segment relation	GLR (GX)	Distance between points G and X.
	IV] Maxillary segments angulations:		
15	Greater segment displacement	GSD (GOT)	Angle between points G, O, and T.
16	Lesser segment displacement	LSD (LOT)	Angle between points L, O, and T.
17	Arch symmetry	AS (IOT)	Angle between points I, O, and T.

Data were explored for normality using *Kolmogorov-Smirnov and Shapiro-Wilk tests*. According to the behavior of the data (either parametric or nonparametric), the suitable statistical test was selected.

The means, standard deviation, and CIs were calculated for each group in each test. For normally distributed data, *independent sample t test* was used to compare between the 2 groups. For each group, *paired sample t test* was used to compare between the 2 time points. Due to the normal distribution of data, the nonparametric tests were not used in the current study.

Results

Participant Flow, Dropouts, and Numbers Analyzed

For D-NAM group, all the 17 infants received the D-NAM appliance. One patient was lost during the follow-up as his family chose to make the follow-ups in another center. Another 2 infants died due to chest infection. The records of the all 14 infants of the D-NAM group were analyzed. While in the control group, 17 infants were allocated. Two infants passed away, one due to chest infection and the other due to a cardiac problem. One more infant was lost as his family chose to complete the follow-up in a nearby hospital. The records of the all 14 infants of the control group were analyzed (Figure 5).

Recruitment

The first infant was allocated in November 13, 2016, while the last infant started treatment in September 9, 2018. All the patients were followed for 3 months.

Baseline Data

For the D-NAM group, 14 UCLP were included; 10 of them had the cleft on the left side, and 4 had it on the right side. In this group, the age of the included infants at the start of the treatment was a mean of 12.58 ($\pm$8.24) days including 11 males and 3 females. The control group included 14 UCLP infants divided into 12 infants with left-sided cleft and 2 with right-sided cleft. The control group participants had a mean age was 12.74 ($\pm$7.28) days encompassing 8 males and 6 females. Most of the 28 included infants in the study had cleft on the left side recording ratio 3.66L:1R. Moreover, it was more common in males than females with ratio 2.11M:1F. The mean age of the included infants was 12.79 ($\pm$0.77) days.

Outcomes and Estimation

Intraobserver and interobserver reliability. Intraobserver and interobserver reliability was assessed between 2 readings done by the 2 assessors to the different measurements using the ICC. Acceptable intraobserver reliability and agreement between all the readings (ICC values ranging from 0.752 to 0.990) were found except for the greater segment length, which recorded a weak reliability (ICC = 0.300).

For the interobserver reliability, acceptable reliability was observed for most of the measurements (ICC values ranging from 0.723 to 0.974). Some measurements recorded moderate interobserver reliability; middle cleft width (0.515), posterior arch width (0.547), greater segment length (0.543), and arch symmetry (0.632).

3D-printed nasoalveolar molding group. Most of the models' measurements in the D-NAM group were changed significantly ($P < .05$) while comparing the 2 measured time points (Table 2). This was not the case for the posterior arch width, greater segment position, lesser segment length, anterior arch length, and total arch length, which showed statistically insignificant changes, although their clinical improvement.

Control group. Unlike the D-NAM group, most of the measurements in the control group were insignificantly ($P > .05$) changed between the 2 measured time points (Table 2). Significant changes occurred only in the canine cleft width, anterior arch length, and arch symmetry.

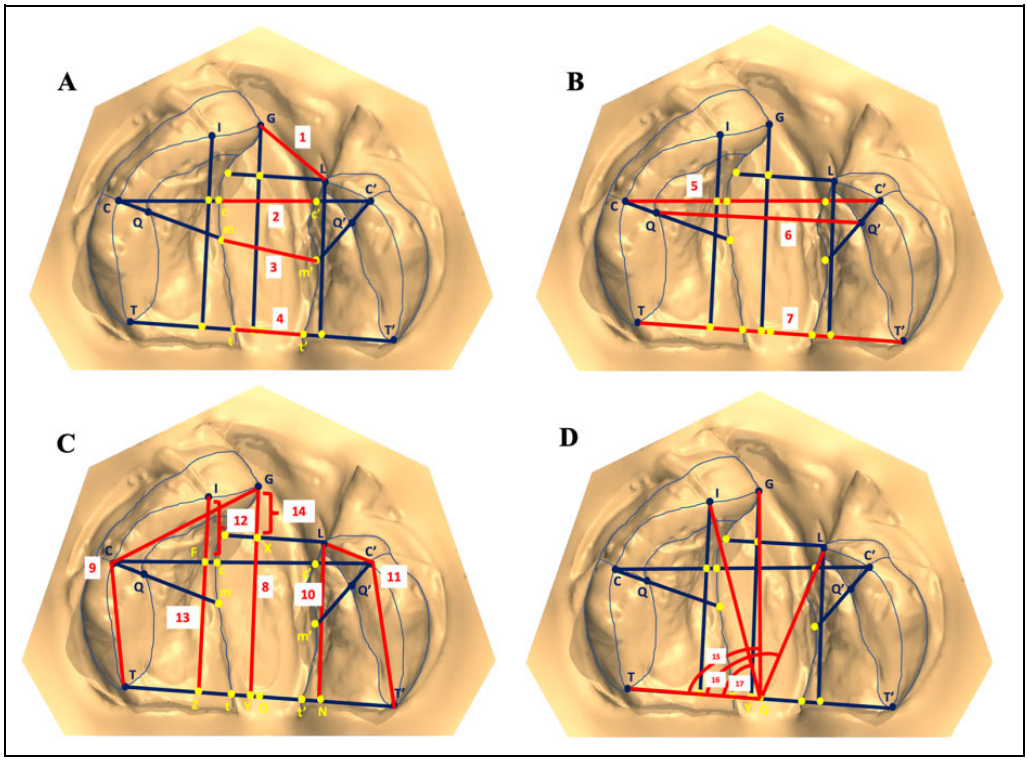

Figure 4. Landmarks (blue); G: greater segment anterior point, L: lesser segment anterior point, I: incisive point, C/C': canine points, Q/Q': gingival groove points and T/T': tuberosity points. Constructed points (yellow); c/c': canine palatal points, m/m': middle palatal points, t/t': posterior palatal points, Z: point Z, Y: point Y, N: point N, X: point X, E: point E, F: point F and O: point O. Cleft widths' measurements (A); 1: anterior, 2: canine, 3: middle, and 4: posterior cleft widths. Arch widths' measurements (B); 5: intercanine region width, 6: middle arch width, and 7: posterior arch width. Anteroposterior measurements (C); 8: greater segment position, 9: greater segment length, 10: lesser segment position, 11: lesser segment length, 12: anterior arch length, 13: total arch length, and 14: greater to lesser segment relation. Maxillary segments angulations (D); 15: greater segment displacement, 16: lesser segment displacement, and 17: arch symmetry.

Differences between the 2 groups. At T2 (difference between T1 and T2), a statistically significant differences were found between the 2 groups in 6 measurements; anterior, canine and middle cleft widths, in addition to greater to lesser segments relation, greater segment displacement, and arch symmetry. Although the rest of the measurements did not statistically differ, an obvious clinical improvement had occurred in the D-NAM group in comparison to the controls (Table 2).

Harms

No harms had occurred related to the D-NAM itself. The most noticeable adverse effect which occurred in this study was related to taping. An obvious amount of irritation and inflammation occurred to most of infants in the area of tape placement. This sometimes developed into an open wound with bleeding.

Discussion

Management of patients with CLP is a long journey, which usually starts at infancy till adulthood. Each trial to make this journey simpler and shorter will be appreciated. The introduced D-NAM technique is a trial to simplify the NAM technique to both the parents and health care providers.

In the D-NAM, not only all the movements were simulated on the virtual model but also complete construction of the intraoral plate was virtually completed. So far, this was considered as the first fully 3D-constructed and 3D-printed intraoral molding plate. The digitized steps were an approach to facilitate the plate activation in a more predictable manner, this is attributed to the full visualization of the final arch form before accepting the amount of activation. Using this capability allowed a more convenient and easy indirect activation of the intraoral plate by altering the digital models. Using a digital software in alveolar segments activations allowed a more accurate activation movements. This was endorsed by the capability of identifying the amount of movement in fraction of millimeters and accurate division of the total amount of cleft gap closure on the applied 3 sequential steps. Although the D-NAM is considered as a more expensive technique than the manual approaches, pretreatment visualization, accurate activation, fast appliances construction (20-30 minutes per patient), and the single button press production through 3D-printing might stand with its usage.

In the current study, ordinary rubber-based impression was made to the included infants, which was then scanned using a desktop scanner to be converted to the virtual models. Direct intraoral scanning to infants is a difficult procedure. Most of

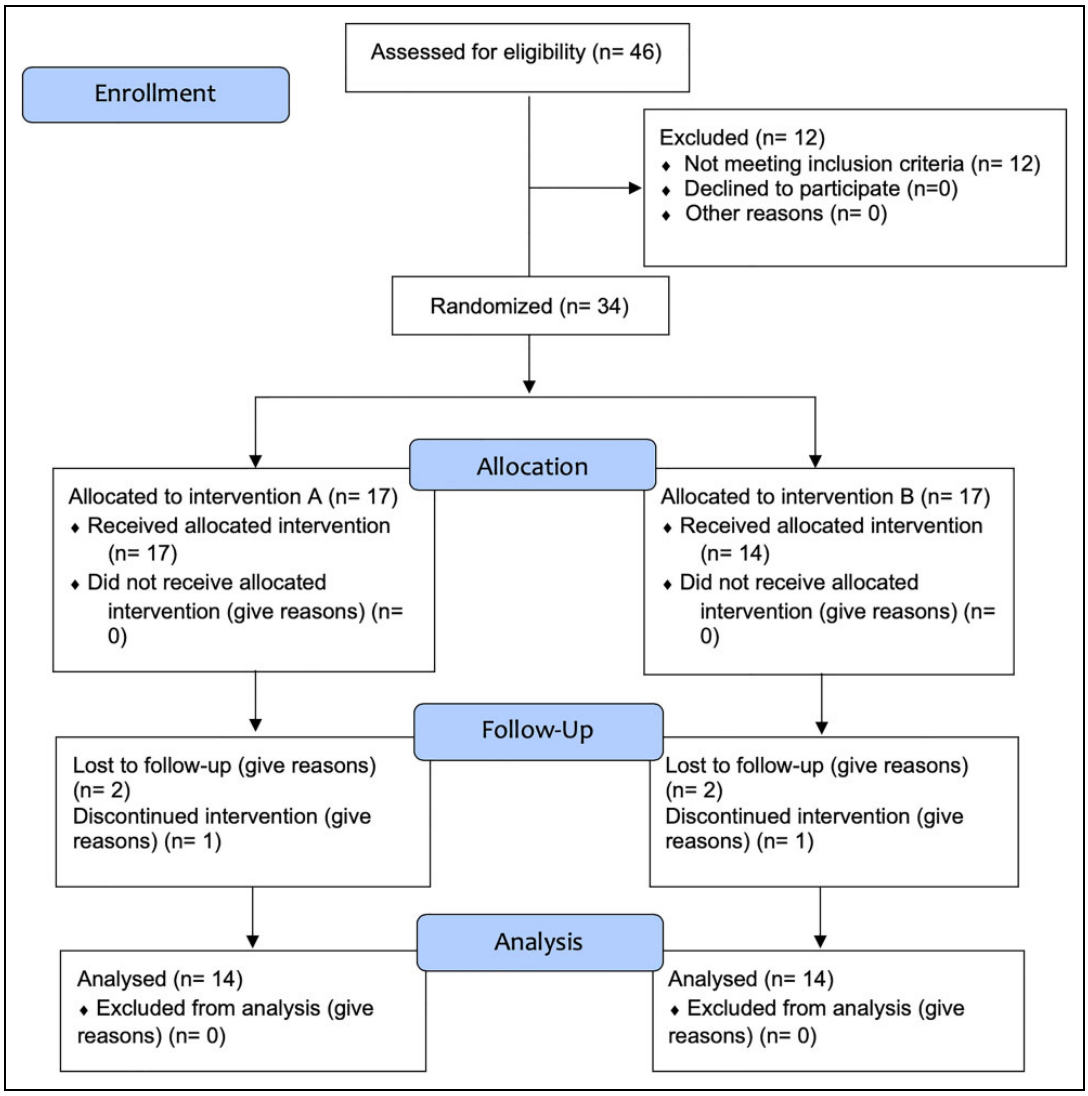

Figure 5. Consolidated Standards of Reporting Trials (CONSORT) flow diagram of the progress through the phases of the current randomized controlled trial (RCT).

the available intraoral scanners are with large head dimensions and they did not allow a proper recording to the infants' maxillary arches, especially when going posteriorly. Another obstacle stands against direct intraoral scanning of the UCLP infants is the scanning time, it is difficult to keep the infant in a still position along the scanning period.

In the current study, the use of the 2 sides tapes with elastics was omitted, which were used for asymmetric force application for cleft gap reduction. The parents usually suffer from fabrication of these 2 sides tapes with the elastics threaded in them. This decision of omission was developed after reaching the results found by the randomized clinical trial done by Chang et al. (2014) in 2014. They compared Grayson's to Figueroa's techniques and found no differences except of more reduction in clefted nostril width with Grayson's technique before the surgery. "This difference was abrogated by surgery" they mentioned. Moreover, the acrylic button was kept in place, although the omission of elastics usage. This acrylic projection facilitates the appliance handling, especially at the beginning of the treatment before nasal stent addition. After nasal stent addition, it protects the wire from distortion by the parents as another handle is present for insertion and removal.

All the previous trials (Yu et al., 2011, 2013; Gong and Yu, 2012; Loeffelbein et al., 2015; Shen et al., 2015; Ritschl et al., 2016) of the CAD/NAM focused on the activation movements and not appliance construction. These trials printed the modified virtual models, then used these models for manual appliance production. In the current study, not only activation of the intraoral plate was virtually performed but also the intraoral plate was virtually constructed then 3D printed. This simple appliance production definitely will facilitate the work of the health care providers and shorten the appointment time. Subsequently, decrease the burden on the infants and their parents.

Table 2. Mean and Standard Deviation of the Different Models' Measurements in the D-NAM and Control Groups at the 2 Time Points, Paired Sample *t* Test Was Used to Compare Between the 2 Time Points in Each Group.[a]

		D-NAM								Control								Difference between the 2 groups at T2 (T1-T2)		
		T1		T2		T1-T2				T1		T2		T1-T2						
	Measurements	Mean	SD	Mean	SD	Mean difference	SD	95% CI	*P* value	Mean	SD	Mean	SD	Mean difference	SD	95% CI	*P* value	Mean difference	95% CI	*P* value
1	Anterior cleft width (mm)	12.81	2.55	6.02	3.12	−6.80	2.50	−8.24 to −5.35	<.001[b]	12.94	3.35	12.85	3.16	−0.10	1.30	−0.81 to 0.62	.781ns	6.70	4.28 to 9.11	<.001[b]
2	Canine cleft width (mm)	12.85	3.11	5.57	2.96	−7.27	2.53	−6.48 to −3.57	<.001[b]	13.00	4.29	11.59	2.97	−1.41	2.38	−2.73 to −0.09	.038[b]	5.85	3.19 to 8.51	<.001[b]
3	Middle cleft width (mm)	13.87	2.50	8.84	3.37	−5.03	2.53	−6.48 to −3.57	<.001[b]	15.21	2.38	14.42	2.31	−0.79	2.43	−2.13 to 0.54	.255ns	4.23	1.62 to 6.84	<.001[b]
4	Posterior cleft width (mm)	13.68	3.66	10.35	3.28	−3.33	3.64	−5.43 to −1.22	.005[b]	15.12	3.27	14.42	2.67	−0.70	2.68	−2.18 to 0.78	.330ns	2.63	−0.83 to 6.10	.197ns
5	Intercanine region width (mm)	31.25	3.86	29.35	4.58	−1.90	3.05	−3.65 to −0.13	.037[b]	31.40	2.64	31.52	2.90	0.12	3.08	−1.58 to 1.83	.878ns	2.02	−1.15 to 5.19	.340ns
6	Middle arch width (mm)	25.91	3.54	24.17	3.99	−1.74	1.57	−2.64 to −0.83	<.001[b]	26.10	2.39	25.40	2.29	−0.70	2.48	−2.07 to 0.67	.292ns	1.03	−1.30 to 3.37	.645ns
7	Posterior arch width (mm)	35.50	4.14	36.23	3.81	0.74	2.27	−0.57 to 2.04	.245ns	36.51	2.36	37.80	2.36	1.28	2.68	−0.20 to 2.76	.085ns	0.54	−2.06 to 3.15	.945ns
8	Greater segment position (mm)	23.86	2.85	23.54	2.70	−0.31	2.94	−2.00 to 1.38	.697ns	23.72	3.56	25.36	2.05	1.64	3.43	−0.25 to 3.54	.084ns	1.95	−1.45 to 5.37	.433ns
9	Greater segment length (mm)	32.66	3.88	36.65	3.67	3.99	4.77	1.23 to 6.74	.008[b]	33.76	4.63	35.74	4.00	1.98	4.59	−0.56 to 4.51	.117ns	−2.01	−6.16 to 2.13	.575ns
10	Lesser segment position (mm)	17.44	2.18	19.77	1.81	2.33	2.23	1.04 to 3.61	.002[b]	17.30	3.01	17.67	2.87	0.38	3.68	−1.66 to 2.41	.698ns	−1.95	−5.11 to 1.20	.364ns
11	Lesser segment length (mm)	23.74	5.25	24.90	2.70	1.16	5.26	−1.87 to 4.20	.423ns	22.00	4.11	23.44	3.67	1.44	3.50	−0.49 to 3.37	.134ns	0.27	−3.70 to 4.25	.998ns
12	Anterior arch length (mm)	8.34	2.20	7.70	1.91	−0.64	2.27	−1.94 to 0.67	.314ns	7.89	1.99	9.02	1.90	1.13	1.08	0.53 to 1.73	.001[b]	1.76	−0.13 to 3.67	.077ns
13	Total arch length (mm)	21.31	3.06	21.82	2.40	0.51	3.17	−1.32 to 2.33	.559ns	21.35	3.17	22.78	2.50	1.44	3.56	−0.53 to 3.40	.140ns	0.93	−2.51 to 4.37	.891ns
14	Greater to lesser segment relation (mm)	6.45	2.13	3.97	2.41	−2.49	2.66	0.95 to 4.01	.004[b]	7.01	3.03	7.75	2.76	0.74	2.31	−0.54 to 2.01	.238ns	3.22	0.75 to 5.68	.006[b]
15	Greater segment displacement (°)	84.24	5.49	97.86	6.75	13.63	7.04	9.56 to 17.69	<.001[b]	86.87	8.77	89.14	9.09	2.27	5.92	−1.01 to 5.54	.161ns	−11.36	−18.35 to −4.36	<.001[b]
16	Lesser segment displacement (°)	115.80	7.04	108.55	7.60	−7.25	7.25	−11.43 to −3.06	.002[b]	118.63	9.55	117.29	8.20	−1.34	5.87	−4.58 to 1.90	.391ns	5.91	−1.37 to 13.19	.150ns
17	Arch symmetry (°)	70.36	5.92	82.99	6.96	12.63	7.78	8.13 to 17.11	<.001[b]	72.44	9.41	76.39	7.95	−3.95	6.63	0.27 to 7.61	.037[b]	3.22	0.75 to 5.68	.006[b]

Abbreviations: D-NAM, 3D-printed nasoalveolar molding; NS, nonsignificant ($P > .05$); SD, standard deviation.

[a]Followed by mean differences and confidence intervals of the different measurements between the 2 groups at T2 (T1-T2), compared using the *independent sample t test*.

[b]Significant ($P < .05$).

Inclusion of an untreated control group in the current study was very helpful as it allowed a full picture visualization of the effectiveness of the introduced new technique.

Limitations

Some unavoidable limitations were present in the current study. One of the important limitations was the parents' cooperation and dedication to the interventions to the D-NAM appliance. Some of the parents omitted the appliance usage without permission to give themselves or their child rest. Once detected, the parents were firmly instructed to stop repeating this attitude. This might be due to the skin irritation that occurred with the tapes. Lack of parents' cooperation was one of the causes of increasing the dropouts to 32.5% in a study done by Rau et al. (2015) in 2015.

Generalizability

Selection of a high-quality study design, following the CONSORT guidelines and calculation of the sample size needed were steps to increase the precision and minimize the amount of bias. Accordingly, this would increase the closeness of the selected sample to the population which is needed to increase the level of generalizability.

Interpretation of the Results

In comparison to the control group, successful results were produced by the D-NAM. A significant improvement (clinically and/or statistically) of all the measured MADs at T2 in comparison to control was detected. The D-NAM was efficient to approximate the 2 maxillary segments, decrease the cleft gap, and improve the arch symmetry. These results matched what was found by Yu et al. (2013) in 2013, Shen et al. (2015), and Loeffelbein et al. (2015) in 2015. It seems that the fully printed intraoral plate was successful and matched the non-printed previous trials. The introduced D-NAM technique is a simpler version of the NAM appliance that can be used to improve the MADs prior to surgical lip repair.

Conclusions

Within the limitation of the current RCT, the following can be concluded:

1. The new D-NAM technique is a successful approach to improve the MADs before surgical lip repair in infants with UCLP.
2. It seems that the fully 3D-printed version of the CAD/NAM can be used as a simpler version of the NAM appliance.

Declaration of Conflicting Interests

The author(s) declared no potential conflicts of interest with respect to the research, authorship, and/or publication of this article.

Funding

The author(s) received no financial support for the research, authorship, and/or publication of this article.

ORCID iDs

Mohamed Abd El-Ghafour, BDS, MSc, PhD, MOrth RCSEd https://orcid.org/0000-0002-0870-1472
Amr Ragab El-Beialy, MSc, PhD, MOrth RCSEd https://orcid.org/0000-0003-1303-3920
Seif El-Din Hegab, BDS, MSc, MOrth RCSEd https://orcid.org/0000-0001-6460-3247

Supplemental Material

Supplemental material for this article is available online.

References

Breitsprecher L, Fanghänel J, Metelmann HR, Mlynski G, Würfel F, Freise K, Knape U. The influence of the muscles of facial expression on the development of the midface and the nose in cleft lip and palate patients. A reflection of functional anatomy, facial esthetics and physiology of the nose. *Ann Anat*. 1999;181(1):19-25.

Brophy TW. Bone surgery essential in the treatment of complete cleft palate. *J Am Dent Assoc*. 1923;10(2):3-18.

Campbell A, Restrepo C, Park E, Navas G, Deshpande G, Swanson J, Bjorn S, Lisa W, Ayala R. Influence of severity on aesthetic outcomes of unilateral cleft lip repair in 1,823 patients. *Plast Reconstr Surg Glob Open*. 2019;7(1):e2083.

Chang CS, Wallace CG, Chien-Jung Pai B, Chiu YT, Hsieh YJ, Chen IJ, Yu-Fang L, Jen-Wein LE, Kuo-Ting Chen P. Comparison of two nasoalveolar molding techniques in unilateral complete cleft lip patients: a randomized prospective single-blinded trial to compare nasal outcomes. *Plast Reconstr Surg*. 2014;134(2):275-282.

Figueroa A, Polley JW. Orthodontics in cleft lip and palate management. In: Mathes SJ, ed. *Plastic Surgery*. 2nd ed. Elsevier; 2006: 271-310.

Friede H, Lilja J. Dentofacial morphology in adolescent or early adult patients with cleft lip and palate after a treatment regiment that included vomer flap surgery and pushback palatal repair. *Scand J Plast Reconstr Surg Hand Surg*. 1994;28(2):113-121.

Gkantidis N, Papamanou D, Karamolegkou M, Dorotheou D. Esthetic, functional, and everyday life assessment of individuals with cleft lip and/or palate. *Biomed Res Int*. 2015;2015:1-8.

Gomez DF, Donohue ST, Figueroa AA, Polley JW. Nasal changes after presurgical nasoalveolar molding (PNAM) in the unilateral cleft lip nose. *Cleft Palate Craniofac J*. 2012;49(6):689-700.

Gong X, Yu Q. Correction of maxillary deformity in infants with bilateral cleft lip and palate using computer-assisted design. *Oral Surg Oral Med Oral Pathol Oral Radiol*. 2012;114(5 suppl): S74-S78.

Grayson B, Cutting C, Wood R. Preoperative columella lengthening in bilateral cleft lip and palate. *Plast Reconstr Surg*. 1993;92(7): 1422-1423.

Hocevar-Boltezar I, Jarc A, Kozelj V. Ear, nose and voice problems in children with orofacial clefts. *J Laryngol Otol*. 2006;120(4): 276-281.

Hoffman J. De Labios leporinos, von Hasenscharte. Bergmann; 1686.

Latham R, Kusy R, Georgiade N. An extraorally activated expansion appliance for cleft palate infants. *Cleft Palate J*. 1976;13: 253-261.

Lisson J, Schilke R, Tränkmann J. Transverse changes after surgical closure of complete cleft lip, alveolus and palate. *Clin Oral Invest*. 1999;3(2):18-24.

Loeffelbein DJ, Ritschl LM, Rau A, Wolff KD, Barbarino M, Pfeifer S, Schönberger M, Wintermantel E. Analysis of computer-aided techniques for virtual planning in nasoalveolar moulding. *Br J Oral Maxillofac Surg*. 2015;53(5):455-460.

Matsuo K, Hirose T, Tomono T, Iwasawa M, Katohda S, Takahashi N, Koh B. Nonsurgical correction of congenital auricular deformities in the early neonate: a preliminary report. *Plast Reconstr Surg*. 1984;73(1):38-50.

McNeil C. Congenital oral deformities. *Br Dent J*. 1956;101(2): 191-198.

Moher D, Hopewell S, Schulz KF, Montori V, Gøtzsche PC, Devereaux PJ, Elbourne D, Egger M, Altman DG. CONSORT 2010 explanation and elaboration: updated guidelines for reporting parallel group randomised trials. *BMJ*. 2010;340(1):c869.

Mossey P, Modell B. Epidemiology of oral clefts 2012: an international perspective. *Front Oral Biol*. 2012;16(2):1-18.

Rau A, Ritschl LM, Mücke T, Wolff KD, Loeffelbein DJ. Nasoalveolar molding in cleft care—Experience in 40 patients from a single centre in Germany. *PLoS One*. 2015;10:e0118103.

Ritschl LM, Rau A, Guell FD, DiBora B, Wolff KD, Schoenberger M, Franz XB, Erich W, Loeffelbein DJ. Pitfalls and solutions in virtual design of nasoalveolar molding plates by using CAD/CAM technology-a preliminary clinical study. *J Craniomaxillofac Surg*. 2016;44(4):453-459.

Ross RB, Mac Namera MC. Effect of presurgical infant orthopedics on facial esthetics in complete bilateral cleft lip and palate. *Cleft Palate Craniofac J*. 1994;31(2):68-73.

Rousseau P, Metzger M, Frucht S, Schupp W, Hempel M, Otten JE. Effect of lip closure on early maxillary growth in patients with cleft lip and palate. *JAMA Facial Plast Surg*, 2013;15(5):369-373.

Schimming R, Hunter NR, Mason KA, Milas L, Bressmann T, Sader R, Horch H. Quality of life research in patients with cleft lip and palate: preliminary results. *Mund Kiefer Gesichtschir*. 1999;3(3):134-139.

Shen C, Yao CA, Magee W, Chai G, Zhang Y. Presurgical nasoalveolar molding for cleft lip and palate: the application of digitally designed molds. *Plast Reconstr Surg*. 2015;135(6):1007e-1015e.

van der Plas E, Koscik TR, Conrad AL, Moser DJ, Nopoulos P. Social motivation in individuals with isolated cleft lip and palate. *J Clin Exp Neuropsychol*. 2013;35(5):489-500.

Yu Q, Gong X, Shen G. CAD presurgical nasoalveolar molding effects on the maxillary morphology in infants with UCLP. *Oral Surg Oral Med Oral Pathol Oral Radiol*. 2013;116(4):418-426.

Yu Q, Gong X, Wang GM, Yu ZY, Qian YF, Shen G. A novel technique for presurgical nasoalveolar molding using computer-aided reverse engineering and rapid prototyping. *J Craniofac Surg*. 2011; 22(1):142-146.

Zhu S, Chen Z. Association between gingival recession and proclination of maxillary central incisors near the cleft in patients with unilateral cleft lip and palate: a retrospective case-control study. *Am J Orthod Dentofacial Orthop*. 2013;143(3):364-370.